J Therm Anal Calorim (2011) 104:1097–1106
DOI 10.1007/s10973-011-1354-7

The pyrolysis of cigarette paper under the conditions that simulate cigarette smouldering and puffing

Shun Zhou · Chenghui Wang · Yingbo Xu · Yuan Hu

Received: 11 May 2010 / Accepted: 18 January 2011 / Published online: 12 February 2011

Abstract The combustion properties and pyrolysis behavior of cigarette paper under the pyrolysis conditions of cigarette smouldering were investigated by micro-scale combustion calorimetry (MCC), thermogravimetric analysis coupled to Fourier transform infrared spectrometer (TG-FTIR), respectively. MCC results demonstrated that the combustion and pyrolysis behavior are influenced by heating rate obviously. TG-FTIR results illustrated that the composition of the gaseous products were mainly composed of CO_2, H_2O carbonyl compounds, CO, and methanol. Flash pyrolysis experiment in combination with high performance liquid chromatography (FPy-HPLC) was used to study the pyrolytic formation of eight carbonyl compounds (i.e., formaldehyde, acetaldehyde, acetone, acrolein, propionaldehyde, crotonaldehyde, methyl ethyl ketone, and butyraldehyde) during the pyrolysis of cigarette paper under the pyrolysis conditions of cigarette puffing. Moreover, the solid char formed after the flash pyrolysis experiments were studied by X-ray photoelectron spectroscopy (XPS). It had been found that the pyrolysis temperature influenced the formation of carbonyl compounds and the composition of char greatly.

Keywords Cigarette paper · TG-FTIR · Flash pyrolysis · Carbonyl compounds · HPLC

S. Zhou (✉) · C. Wang · Y. Xu
Research and Development Centre, China Tobacco Anhui Industrial Corporation, 9 Tianda Road, Hefei 230088, Anhui, People's Republic of China
e-mail: zhous@mail.ustc.edu.cn

Y. Hu
State Key Laboratory of Fire Science, University of Science and Technology of China, 96 Jinzai Road, Hefei 230026, Anhui, People's Republic of China

Introduction

Generally speaking, commercial cigarettes are mainly composed of tobacco shreds, cigarette paper, and filter rod. When the cigarette is smoked, both tobacco shreds and cigarette paper undergo pyrolytic reactions and their products transfer to smoke [1]. Consequently, when assessing the overall chemistry and toxicity of smoke, it is necessary to know the combustion and pyrolysis behavior, especially what pyrolysis products are generated during smoking [2–4].

In the recent years, many papers have been published in the study of the pyrolysis behavior of tobacco constituents and ingredients. For instances, Richard R. Baker et al. from British American Tobacco company, have studied the pyrolysis formation of formaldehyde from sugars and saccharide tobacco ingredients under the experimental conditions that mimic the combustion conditions inside the cigarette burning zone [5–7]. Sharma et al. [8, 9], from Philip Morris, Inc. USA, have investigated the effect of pyrolysis conditions on the formation of polycyclic aromatic hydrocarbons from polyphenolic compounds and the generation of low molecular weight polycyclic aromatic compounds in the pyrolysis of α-amino acids.

Cigarette paper, as an integral part of the cigarette, primarily consists of cellulose, calcium carbonate filler, and little inorganic salts. During smoking process, cigarette paper also undergoes pyrolytic reactions and definitely influences the composition and total volume of pyrolysis products. According to the literatures, many researchers have done a number of experiments in the study of the pyrolysis behavior of cellulose and its derivatives [10–13]. For examples, Camino et al. have studied the thermal decomposition of pure cellulose and pulp paper. Nada et al. have investigated the thermal behavior of cellulose and

some cellulose derivatives. Cullis and co-workers [14] have blended cigarette paper with various inorganic salts and investigated the effect of heating rate on the amount of carbon monoxide. However, as seen from these literatures, there has been little emphasis on the pyrolysis of cigarette paper under the conditions that could simulate cigarette smouldering and puffing. It is well known that unless pyrolysis experiments are performed under dynamic conditions that are pertaining to those that occur during tobacco burning, results can be obtained which have little resemblance to those obtained during cigarette smoking [7]. Recently, a research group, consisted of relevant tobacco scientists from the research centers of cigarette manufacturers operating in Philip Morris, British American Tobacco, Japan Tobacco International, Imperial Tobacco Ltd., etc., has establish a set of pyrolysis conditions which can predict the pyrolytic behavior of tobacco ingredients during smoking. According to their recommendations, the pyrolysis atmosphere between 2 and 20% oxygen could be used to mimic smoking and the pyrolysis experiments should be carried out over a ramped temperature range of preferably 300–900 °C [1].

In this study, micro-scale combustion calorimetry (MCC) and thermogravimetric analysis coupled to Fourier transform infrared spectrometer (TG-FTIR) has been used to investigate the combustion and pyrolysis behavior of cigarette paper under the pyrolysis conditions of cigarette smouldering. Moreover, since carbonyl compounds, especially formaldehyde, acetaldehyde, acetone, acrolein, propionaldehyde, crotonaldehyde, methyl ethyl ketone, and butyraldehyde have been classified as harmful ingredients in cigarette smoke and listed in "Hoffmann analytes" (the "Hoffmann analytes" refers to a list of toxic and carcinogenic constituents in mainstream cigarette smoke compiled by Dr Dietrich Hoffmann) [15, 16], flash pyrolysis experiment in combination with high performance liquid chromatography (FPy-HPLC) has been employed in the determination of the pyrolytic formation of these carbonyl compounds under the pyrolysis conditions of cigarette puffing. In addition, the chemical characters of the solid char formed after the flash pyrolysis experiments are investigated by X-ray photoelectron spectroscopy (XPS).

Experimental

Materials

Cigarette paper (cellulose containing 28–30% calcium carbonate filler and 1.5–4% the mixture of sodium citrate and potassium citrate; permeability = 60 CORESTA units, a CORESTA unit is defined as the airflow rate in cm^3/min under a pressure drop of 1 kPa and divided by the area of paper measured; grammage = 27 g/m^2) was supplied by Minfeng Special Paper Co., Ltd, China. 2, 4-dinitrophenylhydrazine (DNPH) with AR purity was provided by Sinopharm Chemical Reagent Co., Ltd, China. Acetonitrile with 99.99% purity was obtained from TEDIA reagents, Inc., USA. Perchloric acid with AR purity was supplied by Shanghai Jinglu Chemical Reagent Co., Ltd, China. The standard reagents of formaldehyde-DNPH, acetaldehyde-DNPH, propionaldehyde-DNPH, acrolein-DNPH, acetone-DNPH, crotonaldehyde-DNPH, methacrolein-DNPH, butyraldehyde-DNPH were provided by Zhengzhou Tobacco Research Institute of China National Tobacco Corporation.

Measurements

MCC analysis

The MCC measurement was performed by an "MCC-2" micro-scale combustion calorimeter produced by Govmark, Farmingdale, New York. The sample, approximately 4–6 mg, was heated to a specified temperature (i.e., 650 °C) using three different linear heating rates (i.e., 0.5, 2, and 5 °C/s), respectively, in a stream of nitrogen flowing at 90 cm^3/min flow rate. The thermal degradation products were mixed with a 10 cm^3/min stream of oxygen prior to entering a 900 °C combustion furnace. According to the literatures, the above heating rates and experimental atmosphere could simulate the burning conditions inside the burning zone of a smouldering cigarette between puffs [1, 6]. Each sample was run in two replicates and the data presented here were the average of three measurements. The specific heat release rate HRR (W/g) was obtained by dividing dQ/dt (heat release rate) at each point in time by the initial sample mass. The heat of combustion of the fuel gases per unit mass of initial sample HR (J/g) was acquired by time-integration of HRR over the entire test. The temperature, corresponding to the peak heat release rate (PHRR), was defined as ignition temperature [17, 18].

TG-FTIR analysis

Thermogravimetric/infrared spectrometry analysis was performed using TGA Q5000 IR thermogravimetric analyzer that was interfaced to the Nicolet 6700 FTIR spectrophotometer. About 3 mg of cigarette paper was put in an alumina crucible and heated from 40 to 900 °C. In order to simulate the combustion conditions inside the burning zone of a smouldering cigarette between puffs [1, 6], a two-stage temperature program was used for the TGA furnace running under the flow of 5% oxygen in nitrogen and 10% oxygen in nitrogen, respectively: starting temperature 40 °C; initial ramp rate 0.5 °C/s; mid-temperature 300 °C; second ramp rate 3 °C/s; final temperature 900 °C; holding

period 6 s. The pyrolysis products generated from the TGA furnace were introduced into the gas cell of the FTIR analyser by nitrogen with a flow rate at 60 mL/min. The line that transferred the evolved gases from the TGA to the FTIR and the IR cell was maintained at 225 and 230 °C, respectively. The FTIR was operated in the continuous scan mode covering 4000–500 cm^{-1} at a resolution of 4 cm^{-1}.

FPy-HPLC analysis

According to literature [1], the heating rate that occurs in the cigarette burning zone could reach as high as 500 °C/s during cigarette puffing. Due to the limit of heating rate, MCC and TG-FTIR experiments only can mimic the pyrolysis conditions during cigarette smouldering. In order to simulate the pyrolysis conditions during cigarette puffing, the flash pyrolysis method has been chosen. Flash pyrolysis of cigarette paper was performed in a furnace type pyrolyzer, using off-line detections. The detailed arrangement was shown in Fig. 1. It mainly consisted of a tubular heater with a quartz tube reactor inserted in it, a quartz boat used as the sample container, a gas flow controller, a temperature-programming control device, and a product collection system [19, 20]. Prior to the experiments, the pyrolysis quartz tube was heated to 800 °C, and hold for 1 h to remove any contaminants. The flash pyrolysis experiments were carried out at three different temperatures (i.e. 400, 600, and 800 °C), respectively. Detailed experimental procedures were showed as follows. Cigarette paper sample (30 mg) was placed in the quartz boat that firstly rested at an unheated section of the quartz tube, and the relevant outlet was sealed by a self-made airtight valve. When the tube was completely filled with the flow of 10% oxygen in nitrogen (the flow rate of nitrogen was 300 mL/min, the experimental atmosphere was close to the mean oxygen level throughout the pyrolysis and distillation zone inside the burning cigarette during a puff [1]). The quartz boat was rapidly pushed to the flat-temperature zone by the step-pushing pod, and the residence time was 5 min. Then the gaseous products formed in the process of the experiment were transferred into 60-mL DNPH solution. DNPH solution could be obtained as follows: 339.6-mg DNPH was dissolved in 1000-mL acetonitrile firstly and then 1.85-mL perchloric acid was added, diluted with acetonitrile to volume at 2000 mL finally. The carbonyl compounds in the gaseous products could be derivatized well by DNPH due to its high reactivity and selectivity, to form carbonyl-DNPH compounds which could be detected easily by HPLC [21, 22].

HPLC experiments were carried out in an Agilent 1100 Series (USA) instrument. The chromatographic systems primarily consisted of a binary pump, a degasser, an automated injector, a thermostated column compartment and an UV-DAD detector, which were all controlled by Agilent ChemStations. The HPLC experimental procedure was showed as follows. Chromatographic column: Waters Nova-Pak-C18 (4.6 mm × 250 mm, 5 μm), column temperature: 30 °C, column flowrate: 0.8 mL/min, injection volume: 10 μL. Mobile phase A: 100% H_2O; mobile phase B: 100% acetonitrile, detection: 365 nm. Gradient conditions used: 50%A + 50%B (0 min), 50%A + 50%B (20 min), 40%A + 60%B (25 min), 40%A + 60%B (30 min), 20%A + 80%B (35 min), 10%A + 90%B (40 min), 50%A + 50%B (41 min), 50%A + 50%B (45 min). The yields of carbonyl compounds were calculated using a linear calibration curve obtained from the analysis of standard solutions ranging from 0.2 to 100 mg/L. The data presented here were the average of four experimental determinations.

X-ray photoelectron spectroscopy

Then chemical compositions of the residual char formed after the flash pyrolysis experiments were investigated by XPS. The XPS spectra were recorded with a VG Escalab mark II spectrometer (VG Scientific Ltd, UK), using Al Ka excitation radiation (1253.6 eV) and calibrated by assuming the binding energy of carbonaceous carbon to be 284.6 eV.

Results and discussions

MCC analysis

Microscale combustion colorimeter (MCC), as a pyrolysis combustion flow calorimeter using controlled pyrolysis and complete combustion of the fuel gases, can provide a

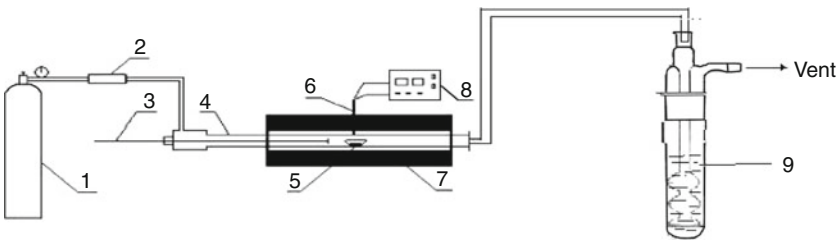

Fig. 1 Set-up of apparatus used in the flash pyrolysis of cigarette paper sample. *1* Gas container; *2* flow meter; *3* handspike; *4* quartz tube; *5* quartz boat; *6* thermocouple; *7* heater; *8* temperature control device; *9* DNPH solution

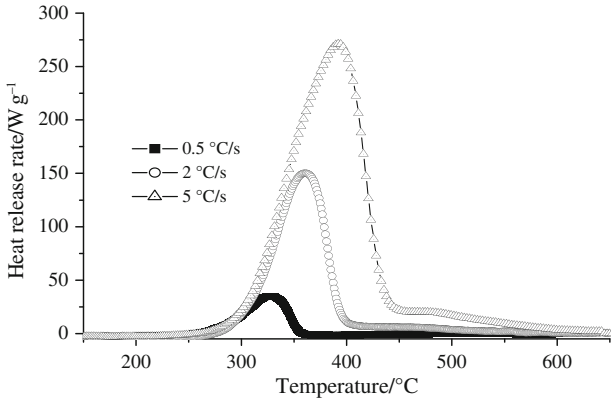

Fig. 2 The HRR versus temperature curves of cigarette paper under different heating rates

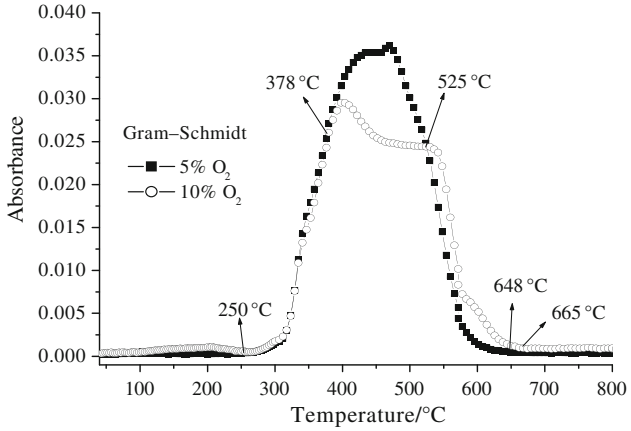

Fig. 4 The Gram–Schmidt curve of the total FTIR absorbance intensity of evolved gaseous products gotten during the pyrolysis process of per milligram cigarette paper by TG-FTIR

Table 1 MCC testing results of cigarette paper

Heating rate/°C s^{-1}	PHRR/W g^{-1}	THR/kJ g^{-1}	IT/°C
0.5	33.5	3.1	320.5
2	150.2	4.6	359.3
5	271.2	5.1	392.1

convenient methodology for evaluating the combustion and pyrolysis properties of materials [17]. Figure 2 shows the HRR versus temperature curves of cigarette paper at different heating rates. The data of peak heat release rate (PHRR), total heat release (THR), and ignition temperature (IT) are listed in Table 1. As shown in Fig. 2 and Table 1, when the heating rate is fixed at 0.5 °C/s, it can be seen that cigarette paper starts to decompose and form fuel gases at 256 °C as shown by an increase in HRR. The HRR curve reaches its maximum (33.5 w/g) at 320 °C (i.e., ignition temperature) and then ends at 360 °C, illustrating that the termination of pyrolytic formation of fuel gases. Moreover, It is noted that the data of PHRR, THR, and IT increase with the increase of heating rate accordingly, indicating that the combustion and pyrolysis behavior are influenced by heating rate obviously.

TG-FTIR analysis

Figure 3a and b presents TG and DTG curves obtained from the pyrolysis of cigarette paper in the atmosphere of 5% and 10% O_2 concentration, respectively. As shown in Fig. 3a, the TG and DTG curves mainly show four weight loss stages. The first stage with a light weight loss of 12.0% takes place in the temperature range of 249–304 °C, corresponding to the thermal decomposition of the mixture of sodium citrate and potassium citrate as well as the partly depolymerization of cellulose with formation of levoglucosan and its evaporation [12, 13]. Then the sharpest weight losing stage could be found in the temperature range from 304 to 425 °C, which may be caused by the extensive thermal degradation of cellulose with the evolution of various gaseous products and the formation of solid char. The following thermal degradation process from 425 to 674 °C is due to the decomposition of char. Finally, the pyrolysis of $CaCO_3$ leads to the appearance of the last weight losing stage in the temperature range of 674–788 °C, and the residual weight at 800 °C is 22.4%. Compared to TG curve in Fig. 3a, TG curve in Fig. 3b also shows four weight loss stages. However, in terms of DTG curves, compared to the case at the lower O_2 concentration,

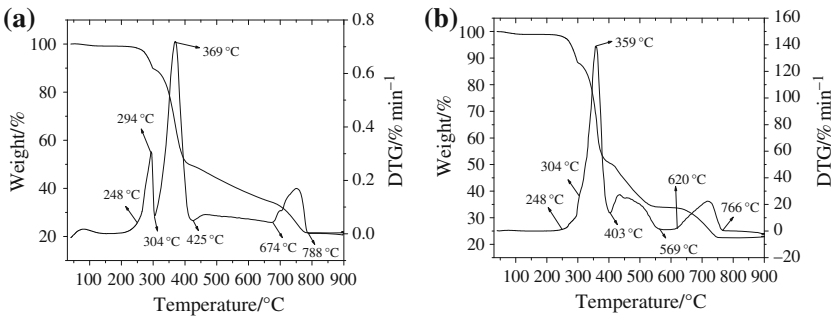

Fig. 3 TG and DTG curves obtained during the pyrolysis process of cigarette paper in the flow of **a** 5% O_2 in nitrogen and **b** 10% O_2 in nitrogen

the first peak at the high O_2 concentration is less visible. Moreover, the temperatures, corresponding to the peak and the end of the second mass loss stage, move toward the low temperature as the O_2 concentration increases form 5 to 10%. This indicates that the increase of O_2 concentration could accelerate the thermal degradation of cellulose. Furthermore, the temperature intervals of the third and fourth weight loss stages shift from 425 to 674 °C and 674 to 788 °C toward 403 to 569 °C and 620 to 766 °C with the increase of O_2 concentration, respectively. This demonstrates that the higher O_2 concentration could catalyze the thermal degradation of the solid char as well as $CaCO_3$.

Figure 4 is the Gram–Schmidt curve of the total FTIR absorbance intensity of gaseous products gotten during the

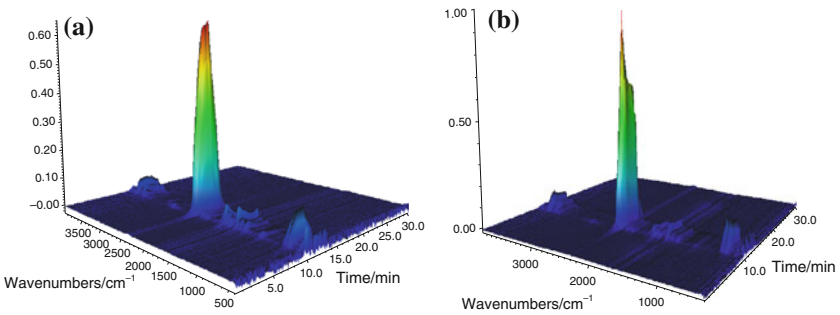

Fig. 5 The 3D surface graph for the FTIR spectra of the gaseous products formed by the pyrolysis of cigarette paper in the flow of **a** 5% O_2 in nitrogen and **b** 10% O_2 in nitrogen

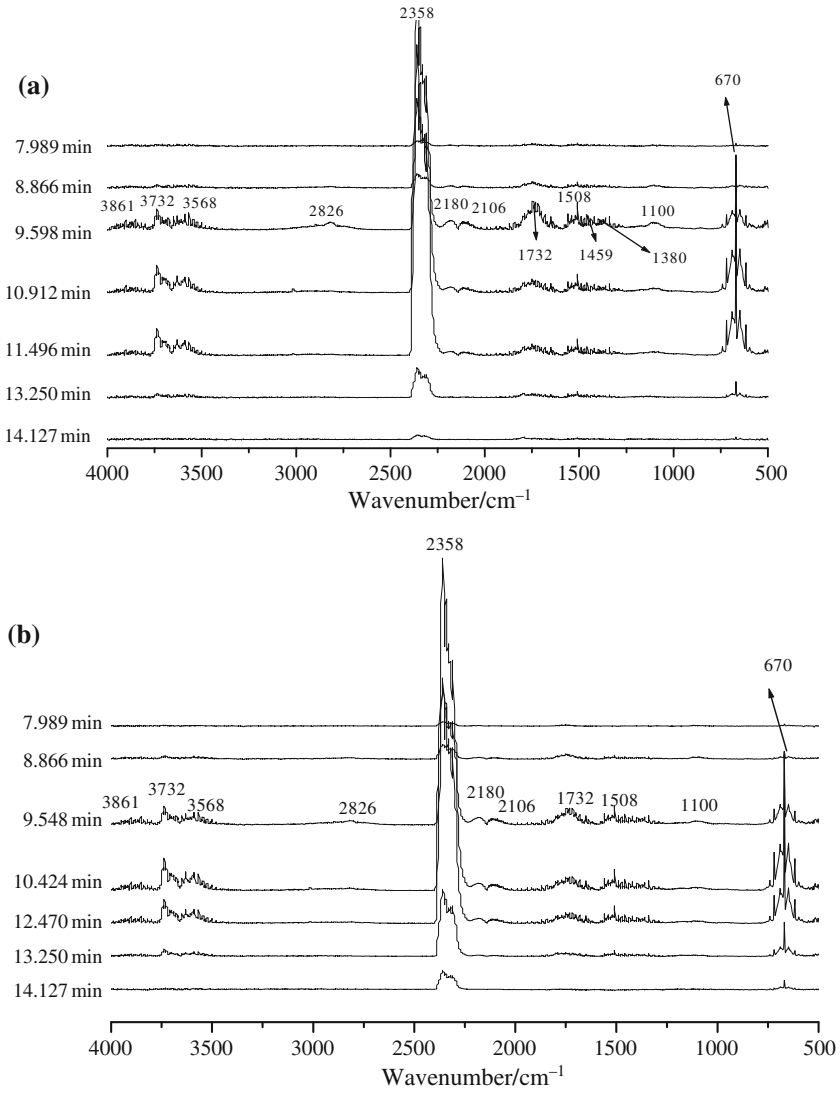

Fig. 6 FTIR spectra of gaseous products obtained at different times during the pyrolysis of cigarette paper in the flow of **a** 5% O_2 in nitrogen and **b** 10% O_2 in nitrogen

pyrolysis process of per milligram cigarette paper by TG-FTIR. As seen from Fig. 4, the gaseous products mainly form in the temperature range of 250–660 °C, which is consistent with the temperature range of weight loss during the thermal decomposition of cigarette paper shown in Fig. 3. Moreover, it can be seen that the total FTIR absorbance intensity obtained in the pyrolysis atmosphere of 5% O_2 is higher than that got in the pyrolysis atmosphere of 10% O_2 when the pyrolysis temperature is in the range of 378–525 °C, illustrating that the formation of gaseous products are influenced by the pyrolysis atmosphere.

The 3D FTIR spectrum (absorbance-wavenumber-minutes) of the gaseous products in the pyrolysis of cigarette paper is showed in Fig. 5. All the pyrolysis products evolved at different times are presented in this FTIR spectrum. It is clear that there are mainly nine absorption regions (i.e., 3770–3450, 3100–2650, 2398–2237, 2230–2000, 1880–1600, 1600–1490, 1490–1255, 1158–1028, and 728–600 cm^{-1}) could be observed from the 3D FTIR spectrum in the time range of 7.79–14.59 min. Figure 6 shows the characteristic FTIR spectra of gaseous products obtained at different times during the pyrolysis of cigarette paper. From Fig. 6a and b, it can be seen that some unambiguous assignments can be adopted. The detection of carbon dioxide in the vicinity of 2358 cm^{-1} is undoubted and it is also confirmed by the peak around 670 cm^{-1}; the attribution of the peaks at 2180 and 2106 cm^{-1} to carbon monoxide is also definite [23]. Furthermore, the absorptions found in the range of 4000–3500 cm^{-1} are well known to be due to –OH groups, which mainly caused by the absorptions of water [24]. Another unambiguous assignment is the peak around 1732 cm^{-1}, which could be ascribed to the C=O group of carbonyl compounds [25].

The absorptions of C–H bonds found nearby 2826, 1459, and 1380 cm^{-1} are normally attributed to hydrocarbons. However, this region of the spectrum is not quite specific, because most of the organic compounds have C–H bonds. As shown in Fig. 3a and b, it is noteworthy that the change tendency of the peak around 1100 (certainly assigned to a C–O bond involving a saturated carbon) is in consistent with those of the peaks at 2826, 1459, and 1380 cm^{-1}, which demonstrates the possibility of the existence of alcohols, in particular methanol [26, 27]. These peaks appear at the time of 9.898 min and disappear at the time of 11.496 min, which principally caused by the pyrolysis of cellulose on the basis of the analysis of TG and DTG curves. Compared Fig. 6b with a, it is noted that no visible differences related the composition of the pyrolysis products could be observed.

The relationship between intensity of characteristic peak and temperature for H_2O, CO_2, CO, and carbonyl compounds is plotted in Fig. 7. It can be seen from Fig. 7 that the release of H_2O, CO_2, CO, and carbonyl compounds mainly occurs in the temperature range of 250–650 °C. In addition, it is obvious that the FTIR intensity of CO_2 is the strongest compared with those of H_2O, CO and carbonyl compounds. As shown in Fig. 7, when the oxygen concentration is increased from 5 to 10%, the FTIR intensity of CO_2, CO, and carbonyl compounds is influenced greatly. In particular, the influence becomes more vigorous with the increase of temperature.

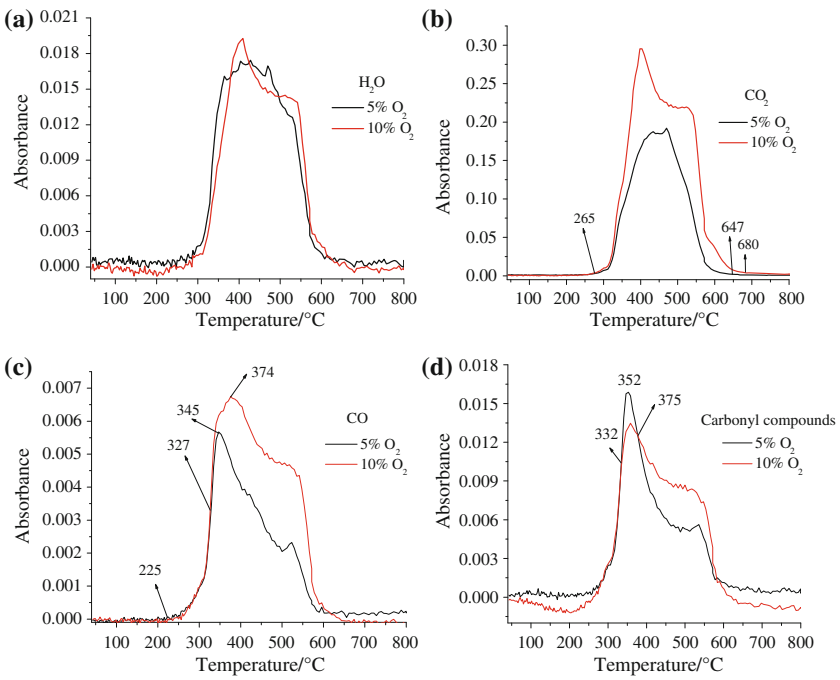

Fig. 7 Relationship between intensity of characteristic peak and temperature for **a** H_2O, **b** CO_2, **c** CO, and **d** carbonyl compounds released by the pyrolysis of per milligram cigarette paper in the flow of 5% O_2 in nitrogen and 10% O_2 in nitrogen

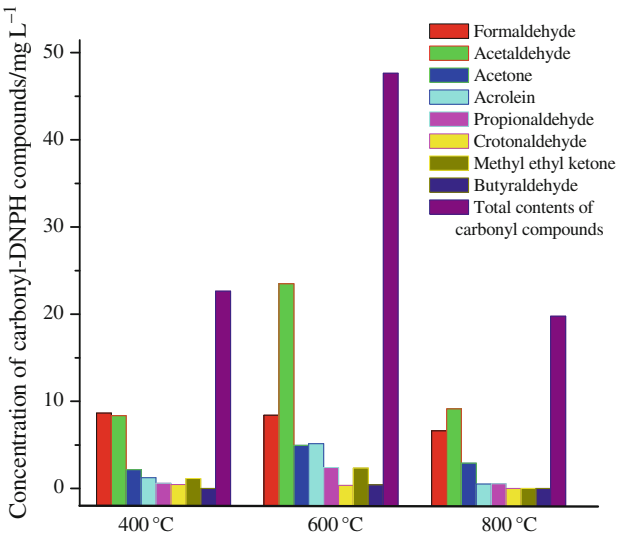

Fig. 8 The individual and total concentration of eight carbonyl compounds formed after the flash pyrolysis of cigarette paper at 400, 600, and 800 °C

Table 2 The composition of carbonyl compounds obtained from the flash pyrolysis of cigarette paper at 400, 600, and 800 °C

Carbonyl compounds (%)	400 °C	600 °C	800 °C
Formaldehyde	38.2	17.7	33.5
Acetaldehyde	36.8	49.3	46.2
Acetone	9.6	10.6	14.7
Acrolein	5.6	10.8	2.7
Propionaldehyde	2.6	5.05	2.8
Crotonaldehyde	2.1	0.75	0
Methyl ethyl ketone	5.1	4.9	0
Butyraldehyde	0	0.9	0

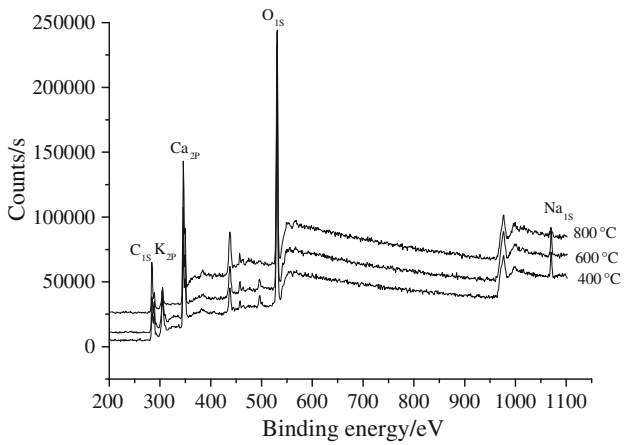

Fig. 9 XPS spectra of the solid char formed after the flash pyrolysis experiments of cigarette paper at 400, 600, and 800 °C

FPy-HPLC analysis

As shown in Fig. 8 and Table 2, eight carbonyl compounds, i.e., formaldehyde, acetaldehyde, acetone, acrolein, propionaldehyde, crotonaldehyde, methyl ethyl ketone, and butyraldehyde could be detected in the gaseous products. According to Fig. 8 and Table 2, it can be seen that the total contents of formaldehyde, acetaldehyde, and acetone account for 84.6% of all detected carbonyl compounds at 400 °C, 77.6% at 600 °C and 94.4% at 800 °C, respectively.

Table 3 XPS results of the char formed after the flash pyrolysis of cigarette paper at 400, 600, and 800 °C

System	Style of residual char/°C	Binding energy/eV
C_{1s}	400	284.6, 286.3, 289.0
	600	284.6, 286.2, 289.0
	800	284.6, 286.2, 289.1
O_{1s}	400	530.84
	600	530.83
	800	530.88
Ca_{2p}	400	346.37
	600	346.34
	800	346.42
K_{2p}	400	292.55
	600	292.43
	800	292.43
Na_{1s}	400	1070.92
	600	1070.86
	800	1071.27

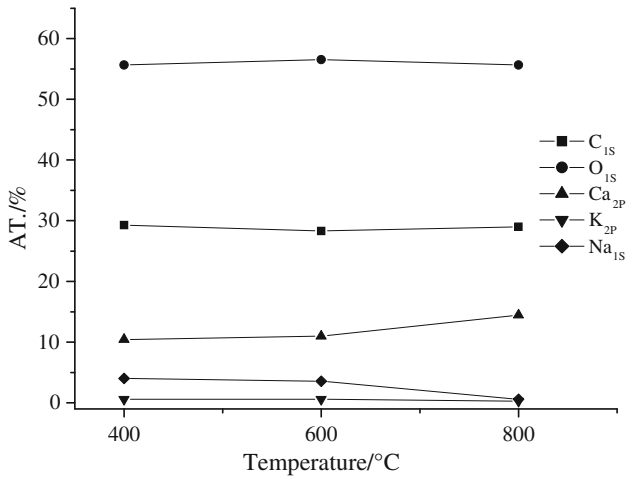

Fig. 10 Changes of the relative contents of elements C, O, Ca, K, and Na in the solid char formed after the flash pyrolysis of cigarette paper at 400, 600, and 800 °C

In the case of formaldehyde, its concentration decrease gradually with the increase of temperature. However, the contents of acetaldehyde and acetone increase firstly when temperature ascends from 400 to 600 °C, and then decrease at 800 °C. It also can be seen from Fig. 8 and Table 2 that crotonaldehyde and methyl ethyl ketone could be detected at 400 and 600 °C, while they can not be found when the temperature is up to 800 °C. By comparison, small amounts of butyraldehyde only could be observed at 600 °C. In addition, it is noteworthy that the total concentrations of the eight carbonyl compounds reach its maximum at 600 °C.

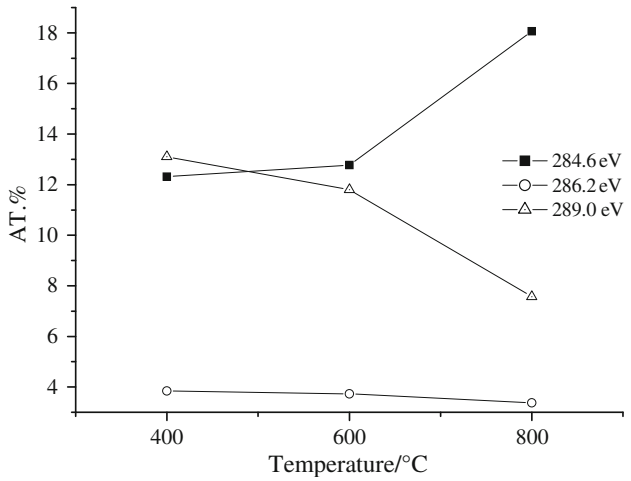

Fig. 11 Changes of the relative contents of elements C with different binding energies in the solid char formed after the flash pyrolysis of cigarette paper at 400, 600, and 800 °C

Chemical analyses of the residual char

The chemical compositions of the solid char formed after flash pyrolysis testing are analyzed by XPS, which is beneficial to understand the pyrolysis behavior of cigarette paper further. Figure 9 shows the XPS spectra of the char formed in the flash pyrolysis experiments of cigarette paper and the assignments are listed in Table 3. As shown in Fig. 9 and Table 3, the peak in the vicinity of 284.6 eV can be assigned to the contribution of C–H and C–C in aliphatic and aromatic species. The peak at 286.0 eV can be ascribed to C–O in cyclized compounds [28, 29]. Moreover, the peaks around 288.9 eV are characteristic of C=O [30]. As for element oxygen, according to the literature, it is impossible to distinguish the inorganic oxygen from the organic oxygen because the O1s band is structureless [31]. The peaks around 530.8 eV could be assigned to the –O– in C–O–C and/or C–OH groups [32, 33]. The peak around 346.3–346.4 eV is due to the Ca_{2p} of element calcium in the $CaCO_3$ structure. The peaks, nearby 292.43–292.55 and 1070.27–1070.92 eV, could be ascribed to Na_{1s} and K_{2p} in their salts (to improve the flammability of cigarette paper, the mixture of sodium citrate and potassium citrate were added in the process of manufacturing), respectively.

The changes of the relative contents of elements C, O, Ca, K, and Na in the residual char of cigarette paper formed after the flash pyrolysis experiments are shown in Fig. 10. It can be seen that the relative contents of elements C and O change little with the change of pyrolysis temperature. However, the atomic percents of Ca increase from 10.45 to 14.45% when temperature increases from 400 to 800 °C.

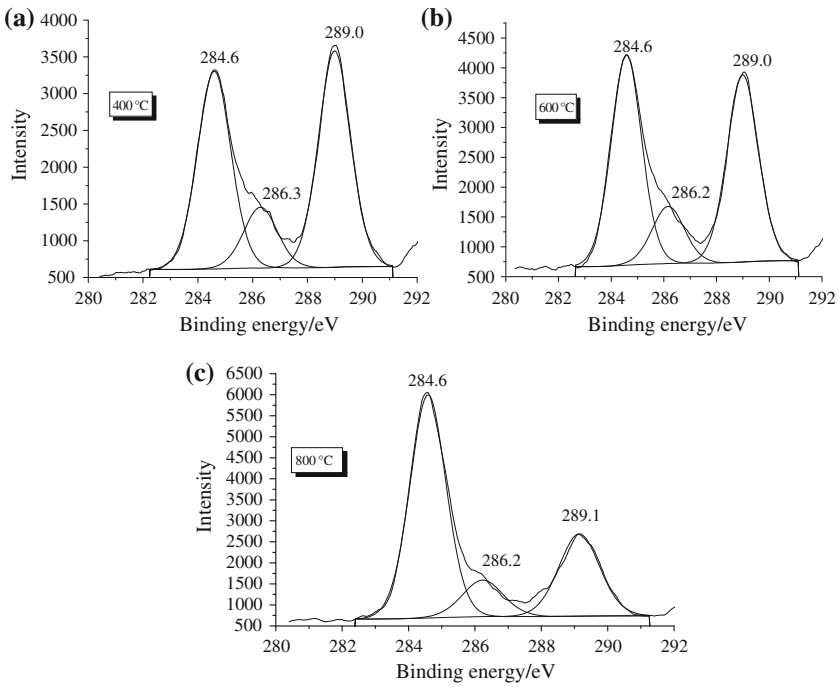

Fig. 12 C_{1s} spectra of the residual char of cigarette paper formed after flash pyrolysis at **a** 400 °C, **b** 600 °C, and **c** 800 °C

This is due to that the thermal decomposition of $CaCO_3$ when the temperature is higher than 600 °C, leading to the release of CO_2 and formation of CaO which is thermally stable at 900 °C. Meanwhile, the relative contents of elements Na and K decrease from 0.6 and 4.03% to 0.27 and 0.6%, respectively, demonstrating the thermal decomposition of sodium citrate and potassium citrate. Of the most interest is the change of element C with different binding energies. As shown in Fig. 11, with the increase of temperature, the atomic percents of elements C in C–H and/or C–C bonds, increases from 12.32 to 18.06, while the atomic percents of elements C in C–O and C=O bonds decrease from 3.84 and 13 to 3.37 and to 7.57, respectively. Moreover, as seen from Fig. 12, the relative intensity ratio of C–C/C–O and C–C/C=O increase with the increase of temperature. According to literatures [34, 35], the solid residue formed at 400 °C may be partly composed of polyaromatic structures. These polyaromatic structures are grafted by many groups such as aliphatic, ether and ketonic groups which can be used to create links and loops between various aromatic clusters. When the pyrolysis temperature increases, these groups will be partly destroyed, with the release of various gaseous products. Meanwhile, the polyaromatic structures could stack compactly further.

Conclusions

In this study, MCC results demonstrate that the data of peak heat release rate, total heat release, and ignition temperature is influenced by the change of heating rate obviously. The TG-FTIR curves show that the pyrolysis process of cigarette paper mainly consists of four stages and the gaseous products are principally composed of CO_2, H_2O, CO, methanol, and carbonyl compounds. The flash pyrolysis in combination with HPLC technique has been used to study the formation of carbonyl compounds under the pyrolysis conditions of cigarette puffing. It has been found that formaldehyde, acetaldehyde, and acetone account for the most part of the carbonyl compounds at the pyrolysis temperature of 400, 600, and 800 °C. According to XPS results, it is noted that the chemical compositions of the solid char formed after the flash pyrolysis of cigarette paper vary with the change of pyrolysis temperature.

Acknowledgements The financial support from China Tobacco Anhui Industrial Corporation (No: 20111004) is acknowledged. The authors wish to thank Dr. Yiwei Xing, Xin Wang and Yongchun Kan (state key laboratory of fire science, university of science and technology of China) for their valuable assistance and suggestions on this manuscript. Gratitude is also expressed to our colleagues Qing He, Gang Chen and Dongliang Zhu for their beneficial help.

References

1. Baker RR, Bishop LJ. The pyrolysis of tobacco ingredients. J Anal Appl Pyrolysis. 2004;71(1):223–311.
2. Baker RR, Massey ED, Smith G. An overview of the effects of tobacco ingredients on smoke chemistry and toxicity. Food Chem Toxicol. 2004;42(1):53–83.
3. Baker RR, Pereira da Silva JR, Smith G. The effect of tobacco ingredients on smoke chemistry. Part I: flavourings and additives. Food Chem Toxicol. 2004;42(1):3–37.
4. Baker RR, Pereira da Silva JR, Smith G. The effect of tobacco ingredients on smoke chemistry. Part II: casing ingredients. Food Chem Toxicol. 2004;42(1):39–52.
5. Baker RR, Coburn S, Liu C. The pyrolytic formation of formaldehyde from sugars and tobacco. J Anal Appl Pyrolysis. 2006;77(1):12–21.
6. Baker RR, Coburn S, Liu C, Tetteh J. Pyrolysis of saccharide tobacco ingredients: a TGA–FTIR investigation. J Anal Appl Pyrolysis. 2005;74(1–2):171–80.
7. Baker RR, Bishop LJ. The pyrolysis of non-volatile tobacco ingredients using a system that simulates cigarette combustion conditions. J Anal Appl Pyrolysis. 2005;74(1–2):145–70.
8. Sharma RK, Chan WG, Seeman JI, Hajaligol MR. Formation of low molecular weight heterocycles and polycyclic aromatic compounds (PACs) in the pyrolysis of α-amino acids. J Anal Appl Pyrolysis. 2003;66(1–2):97–121.
9. Sharma RK, Hajaligol MR. Effect of pyrolysis conditions on the formation of polycyclic aromatic hydrocarbons (PAHs) from polyphenolic compounds. J Anal Appl Pyrolysis. 2003;66(1–2):123–44.
10. Kim UJ, Eom SH, Wada M. Thermal decomposition of native cellulose: influence on crystallite size. Polym Degrad Stab. 2010;95(5):778–81.
11. Nada AMA, Hassan ML. Thermal behavior of cellulose and some cellulose derivatives. Polym Degrad Stab. 2000;67(1):111–5.
12. Gaan S, Rupper P, Salimova V, Heuberger M, Rabe S, Vogel F. Thermal decomposition and burning behavior of cellulose treated with ethyl ester phosphoramidates: effect of alkyl substituent on nitrogen atom. Polym Degrad Stab. 2009;94(7):1125–34.
13. Soares S, Camino G, Levchik S. Comparative study of the thermal decomposition of pure cellulose and pulp paper. Polym Degrad Stab. 1995;49(2):275–83.
14. Baldry PJ, Cullis CF, Goring D, Hirschler MM. The combustion of cigarette paper. Fire Mater. 1988;12(1):25–33.
15. Miyake T, Shibamoto T. Quantitative analysis by gas chromatography of volatile carbonyl compounds in cigarette smoke. J Chromatogr A. 1995;693(2):376–81.
16. Blot WJ, Fraumeni JF. Cancers of lung and pleura in cancer epidemiology and prevention. New York: Oxford University Press; 1996.
17. Lyon RE, Walters RN. Pyrolysis combustion flow calorimetry. J Anal Appl Pyrolysis. 2004;71(1):27–46.
18. Hergenrother PM, Thompson CM, Smith JG, Connell JW, Hinkley JA, Lyon RE, Moulton R. Flame retardant aircraft epoxy resins containing phosphorus. Polymer. 2005;27(14):5012–24.
19. Hu YH, Li SF. The effects of magnesium hydroxide on flash pyrolysis of polystyrene. J Anal Appl Pyrolysis. 2007;78(1):32–9.
20. Han DL, Wang TF, Lin ZK, Hu YH, Zhao FQ, Yi JH, Li SF. Promoting effects of polyacrylamide on ignition and combustion of Al/H2O based fuels: experimental studies of polyacrylamide aqueous solution flash pyrolysis. J Anal Appl Pyrolysis. 2010;87(1):56–64.
21. Long WJ, Henderson JW. Rapid separation and identification of carbonyl compounds by HPLC. Agilent Technologies, Publication No. 5988-6346EN (2002).

22. Schulte E. Determination of higher carbonyl compounds in used frying fats by HPLC of DNPH derivatives. Anal Bioanal Chem. 2002;372(5–6):644–8.
23. Anca MM, Lucia O, Apostolescu N, Moldoveanu C. TG-FTIR study on thermal degradation in air of some new diazoaminoderivatives. J Therm Anal Calorim. 2010;100(2):615–22.
24. Buryan P, Staff M. Pyrolysis of the waste biomass. J Therm Anal Calorim. 2008;93(2):637–40.
25. Loría-Bastarrachea MI, Herrera-Kao W, Cauich-Rodríguez JV, Cervantes-Uc JM, Vázquez-Torres H, Ávila-Ortega A. A TG/FTIR study on the thermal degradation of poly (vinyl pyrrolidone). J Therm Anal Calorim. 2010. doi: 10.1007/s10973-010-1061-9.
26. Biagini E, Barontini F, Tognotti L. Devolatilization of biomass fuels and biomass components studied by TG/FTIR technique. Ind Eng Chem Res. 2006;45(13):4486–93.
27. Bruno SS, Ana PDM, Ana MRFT. TG-FTIR coupling to monitor the pyrolysis products from agricultural residues. J Therm Anal Calorim. 2009;97(2):637–42.
28. Wang JQ. Theory of X-ray photoelectron spectroscopy. Beijing: Industry of National Defence Press; 1992.
29. Nakayama Y, Soeda F, Ishitani A. XPS study of the carbon fiber matrix interface. Carbon. 1990;28(1):21–6.
30. Gonzalez-Elipe AR, Martinez-Alonso A, Tascon JMD. XPS characterization of coal surfaces: study of aerial oxidation of brown coals. Surf Interface Anal. 1988;12(12):565–71.
31. Delpeux S, Beguin F, Benoit R, Erre R, Manolova N, Rashkov I. Fullerene core star-like polymer-1: preparation from fullerenes and monoazidopolyethers. Eur Polym J. 1998;34(7):905–15.
32. Brown NMD, Hewitt JA, Meenan BJ. X-ray-induced beam damage observed during X-ray photoelectron spectroscopy (XPS) studies of palladium electrode ink materials. Surf Interface Anal. 1992;18(3):187–98.
33. Shih PY, Yung SW, Chin TS. Thermal and corrosion behavior of P_2O_5-Na_2O-CuO glasses. J Non-Cryst Solids. 1998;224(2):143–52.
34. Bourbigot S, Michel LB, Gengembre L, Delobel R. XPS study of an intumescent coating: application to the ammonium polyphosphate/pentaerythritol fire-retardant system. Appl Surf Sci. 1994;81(1):299–307.
35. Sharma RS, Wooten JB, Baliga VL, Hajaligol MR. Characterization of chars from biomass-derived materials: pectin chars. Fuel. 2001;80(1):1825–36.